Electro-Membrane Filtration for the Selective Isolation of Bioactive Peptides From an α_{s2}-Casein Hydrolysate

Gerrald Bargeman,[1] Joukje Houwing,[1] Isidra Recio,[2] Geert-Henk Koops,[3] Caroline van der Horst[1]

[1]NIZO Food Research, P.O. Box 20, 6710 BA Ede, The Netherlands
[2]Instituto de Fermentaciones Industriales (CSIC), Juan de la Cierva, 3, 28006 Madrid, Spain
[3]University of Twente, Faculty of Chemical Technology, P.O. Box 217, 7500 AE Enschede, The Netherlands

Received 7 September 2001; accepted 14 May 2002

DOI:10.1002/bit.10419

Abstract: For the isolation of the ingredients required for functional foods and nutraceuticals generally membrane filtration has too low a selectivity and chromatography is (too) expensive. Electro-membrane filtration (EMF) seems to be a breakthrough technology for the isolation of charged nutraceutical ingredients from natural sources. EMF combines the separation mechanisms of membrane filtration and electrophoresis. In this study, positively charged peptides with antimicrobial activity were isolated from an α_{s2}-casein hydrolysate using batch-wise EMF. α_{s2}-Casein f(183–207), a peptide with strong antimicrobial activity, predominated in the isolated product and was enriched from 7.5% of the total protein components in the feed to 25% in the permeate product. With conventional membrane diafiltration using the same membrane (GR60PP), isolation of this and other charged bioactive peptides could not be achieved. The economics of EMF are mainly governed by the energy costs and the capital investment, which is affected by the flux of the desired peptide. A maximum average transport rate of α_{s2}-casein f(183–207) during batch-wise EMF of 1.2 g/m^2 · h was achieved. Results indicate that an increase in the hydrolysate (feed) concentration, the applied potential difference and the conductivity of the permeate and electrode solutions, and a reduction in the conductivity of the feed result in a higher transport rate of α_{s2}-casein f(183–207). This is in line with the expectation that the transport rate is improved when the concentration, the electrical field strength, or the electrophoretic mobility is increased, provided that the electrophoretic transport predominates. The expected energy consumption of the EMF process per gram of peptide transported was reduced by approximately 50% by applying a low overall potential difference and by processing desalinated hydrolysate. Considerable improvements in transport rate, energy efficiency, and process economics seem to be attainable by additional optimization of the process parameters and the EMF module design. © 2002 Wiley Periodicals, Inc. *Biotechnol Bioeng* **80:** 599–609, 2002.

Keywords: electro-membrane filtration; isolation; electrophoresis; peptides; bioactive; nutraceutical

INTRODUCTION

In the food industry, there is a clear trend towards the production of so-called functional foods and nutraceuticals. Biologically active ingredients from natural sources are held responsible for the health- and well-being-promoting effects of these products. Various biological activities have been shown for many peptides, particularly for those of dairy protein origin (Gill et al., 1996; Meisel and Schlimme, 1996). Metal-transporting (phosphopeptides) and antimicrobial peptides are usually strongly charged. The presence of this charge is thought to be essential for their biological activity (Recio and Visser, 1999).

For the isolation of these natural ingredients from usually complex feeds containing various hydrolyzed protein fractions of similar size, generally membrane filtration has too low a selectivity whereas chromatography is (too) expensive. Since the production of a mixture of charged bioactive ingredients is usually sufficient for product applications, electro-membrane filtration (EMF) seems to be a promising alternative technology. EMF combines conventional membrane filtration (microfiltration, ultrafiltration, or nanofiltration) with electrophoresis. Compared to pressure-driven membrane filtration, an increase in selectivity for the isolation of charged components is therefore anticipated.

The electrical field was originally introduced in membrane modules to reduce membrane fouling or concentration polarization (Pupanat et al., 1998; Radovich and Behnam, 1983; Rios et al., 1988; Rios and Freud, 1991; Wakeman, 1998; Yukawa et al., 1983; Zumbusch et al., 1998), thereby maintaining a high permeate flux.

Contract grant sponsor: Dutch Programme on Ecology, Economy and Technology (E.E.T.)

Correspondence to: Gerrald Bargeman, NIZO Food Research, Kernhemseweg 2, Ede 6710 BA, The Netherlands.

In more recent studies, the electrical field strength was used as primary driving force to enhance the separation efficiency for the isolation of charged components (e.g., Lentsch et al., 1993; Robinson et al., 1993). In most publications (Bargeman et al., 2000; Daufin et al., 1995; van Nunen, 1997) the selective isolation of amino acids and proteins from synthetic feedstocks is reported. Only a few studies deal with the isolation of valuable charged components from industrially available feeds. The isolation of antibodies from ascitic fluids on an analytical scale and of amino acids and bioactive components from hydrolysates are described by Lim et al. (1998) and Bargeman et al. (2000), respectively.

In this article the technological feasibility of EMF for the isolation of a product enriched in positively charged antimicrobial peptides and especially in α_{s2}-CN f(183–207), a proven bioactive peptide, from a complex α_{s2}-casein (α_{s2}-CN) hydrolysate is studied, validated, and compared with conventional ultrafiltration. The economic feasibility of EMF for industrial applications is mainly determined by the capital investments in the installation, the membranes and the electrodes, and the energy costs (van Nunen, 1997). Since the required capital investment is strongly related to the transport rate of the desired product through the membrane, the effect of process parameters on the transport rate and the energy efficiency during EMF is investigated and reported. These results provide the required information for a process cost estimate of EMF.

Theoretical Aspects

The principle of EMF is illustrated schematically in Fig. 1. Besides conventional membranes, ion-exchange (IEX) membranes are used to prevent degradation of the feedstock and the permeate (usually the product) by preventing direct contact with the electrodes. EMF therefore resembles electrodialysis (ED). The main difference is the use of a conventional microfiltration (MF), ultrafiltration (UF), or nanofiltration (NF) membrane to allow the transport (selective isolation) of components of larger size (e.g., peptides) than usually achieved by ED from the feed to the permeate (or product) compartment. Apart from the desired transport of peptides, small salt ions are also transported as a consequence of the applied potential difference (see Fig. 1).

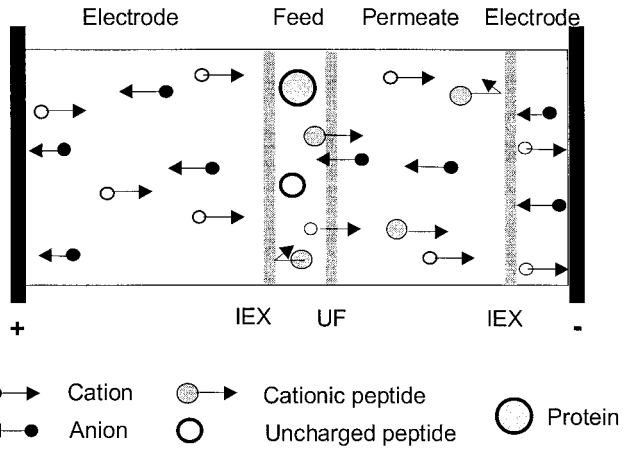

Figure 1. Principle of electro-membrane filtration for selective transport of positively charged (cationic) peptides from the feed to the permeate compartment through an UF membrane.

As in ED, limiting-current effects may occur, when the transport rate of ions toward the IEX membrane by diffusion is lower than the required electrophoretic transport of ions through the membrane (van Nunen, 1997). Thus depletion of ions in the film layer of the membranes may occur, resulting in an increase of the electrical resistance of this layer. When this situation arises, water splitting will occur to maintain the current. Both water splitting and depletion of ions in the film layer will reduce the energy efficiency of the process. Furthermore, water splitting may result in strong changes of the pH of the electrode solutions, the feedstock, and the permeate. Factors influencing the occurrence of limiting-current situations include the salt concentration of the solutions, the cross-flow velocity in the compartments, and the position of the cation- and anion-exchange membranes in relation to the position of the anode and cathode (van Nunen, 1997).

The transport of components through the UF membrane during EMF can be described by Maxwell–Stefan (e.g., Straatsma et al., 2002) or extended Nernst–Planck models (Schlögl, 1966). To get a quick impression of the parameters that may influence the transport rate and the separation selectivity, the extended Nernst–Planck equation is very suitable:

$$J_i = k_i v c_i - D_i \frac{\partial c_i}{\partial x} + F\, z_i c_i u_i E_f \qquad (1)$$

The separation selectivity for the isolation of charged (antimicrobial) components is maximized when the transport rate of the charged components is maximized relative to the transport rate for neutral components. This can be achieved by minimizing the convective (kvc) and diffusive ($-D\frac{\partial c}{\partial x}$) transport. On the basis of Eq. (1), a high selectivity can therefore be achieved by maximizing the electrical field strength E and the electrophoretic mobility u and minimizing the trans-membrane pressure over the UF membrane. Selection of the optimal molecular weight cut-off of the membrane can furthermore exclude possible undesired large components. The transport rate for any component can be increased (up to the concentration where concentration polarization or membrane fouling starts to occur) when the concentration c in the feedstock compartment is increased.

The electrical field strength in the feed compartment cannot be controlled independently but results from the total potential difference applied, liquid resistances in the electrode, permeate and feed solutions, and membrane-related resistances. These latter include resistances in the stationary diffusion film layer at the membrane surface and the resistance of the membranes.

The electrophoretic mobility u is related to the diffusivity of the component. At low ionic strength of the feed solution, the diffusivity of charged peptides and proteins is reduced due to a lack of counter-ions and retardation of the transport through the membrane may occur.

MATERIALS AND METHODS

Feedstocks

Production of α_{s2}-Casein Hydrolysate

A solution enriched in α_{s2}-casein was prepared from sodium caseinate (DMV, The Netherlands) as described by Vreeman and van Riel (1990), only using a single precipitation step. An 8% (m/v) solution of sodium caseinate in double-distilled water was treated with 1.2% (m/m of caseinate) dithiothreitol (Sigma, St. Louis, MO). The pH was adjusted to 6.5 by addition of 2 *M* HCl. 1-Propanol (J.T. Baker, Deventer, The Netherlands) was added to a final concentration of 40% propanol (v/v) while stirring. The solution was left overnight at 2°C. The particles in the resulting suspension were collected by centrifugation at 27,300*g* for 35 min. The supernatant was decanted and drained from the pellets, which were washed once with 1-propanol. The pellet obtained was dissolved in water. The propanol residue was removed from this solution by rotary-evaporation under vacuum. The enriched solution contained approximately 25% of α_{s2}-casein, as judged from the peak areas determined by analytical reversed-phase (RP)-HPLC.

A 2% (m/v) aqueous solution of the enriched α_{s2}-casein solution was adjusted to pH 2.5 using 1 *M* HCl and digested with 6% (m/m of substrate) porcine pepsin A (EC 3.4.23.1, 439 units/mg solid) for 4 h at 37°C in a water bath under agitation. The hydrolysis reaction was terminated by a heat treatment at 85°C for 15 min. After cooling, the pH of the digest was adjusted to 7.0 by addition of 1 *M* NaOH, and the solution was centrifuged at 16,300*g* for 15 min. The supernatant was freeze-dried and stored at 4°C. Three different batches of hydrolysate were produced (respectively hydrolysate A, hydrolysate B, and hydrolysate C), with marginally different peptide concentrations.

Production of Desalinated α_{s2}-Casein Hydrolysate

A solution containing approximately 10 g/L hydrolysate B was desalinated by diafiltration with NF40 membranes (Filmtech) at 20°C and 20 bar inlet pressure using reverse osmosis (RO) water. Thus, the conductivity of the α_{s2}-casein hydrolysate solution was reduced from 2,750 μS/cm (hydrolysate B) to 970 μS/cm (hydrolysate D). The desalinated solution was freeze-dried and stored at 4°C.

Feedstock Solutions

The feed solution for the experiments was prepared by dissolving the freeze-dried hydrolysate (A, C, or D) in RO water. To ensure that the solutions of hydrolysates A and D had a similar peptide concentration, the hydrolysate D solutions were prepared based on an absorbance at 280 nm (A_{280}) equal to those for the hydrolysate A solutions. Before the EMF experiments the pH was adjusted to 8.0.

Membranes

During the ultrafiltration/diafiltration and the EMF experiments, a flat sheet polysulphone membrane, GR60PP (DOW, Filmtech) with a molecular weight cut-off of 25Da was used. This molecular weight cut-off is approximately 8 times the molecular mass of α_{s2}-CN f(183–207), the target peptide for isolation. The installed membrane area was 0.036 and 0.008 m^2 for diafiltration and EMF experiments, respectively. During EMF furthermore CMX and AMX (Tokoyama Soda) IEX membranes were used.

Ultrafiltration Equipment and Conditions

A 2.5 g/L hydrolysate C solution was diafiltered continuously with RO permeate in a DDS lab-20 system (van der Horst et al., 1995). Diafiltration was done at $T = 20$°C, $P = 10$ bar (inlet pressure), pH 7.0, and a cross-flow velocity of approximately 0.9 m/s. In total a diafiltration water volume five times the initial feedstock volume was used (500% DF). Momentary samples taken after 50 min of operation (at 170% DF) were analyzed for the peptide content.

Electro-membrane Filtration Experiments

A schematic representation of the EMF equipment used is presented in Fig. 2. The EMF rig consists of a feedstock/concentrate compartment (C), a permeate (or product) compartment (P), and two electrode compartments (El). The volumes of the feedstock, permeate, and electrode compartments (including supply vessel and piping volume) were 2.5 L, between 1.15 and 1.35 L, and between 1 and 10 L,

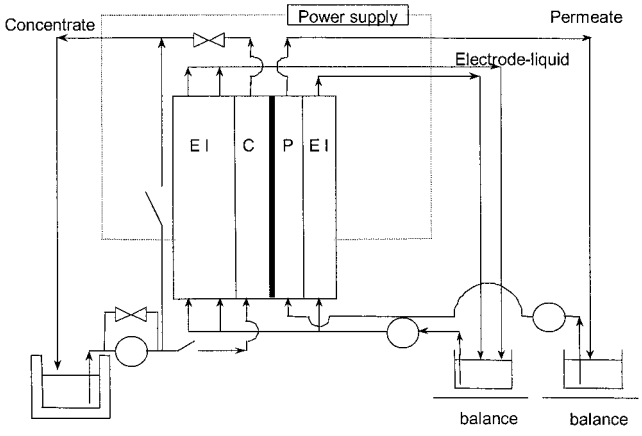

Figure 2. Experimental batch-wise EMF system. Feedstock/concentrate, permeate and electrode solutions are recycled over the concentrate (C), permeate (P), and electrode (El) compartments, respectively.

respectively. The rig was operated batch-wise. Neither concentrate nor permeate was withdrawn from the rig during the experiments, apart from sampling for product analysis. The trans-membrane pressure over the GR60PP membrane, separating the feed compartment from the permeate compartment, at the inlet was minimized (0.1 bar) to reduce the transport by convection to a minimum, thereby maximizing the selectivity of the separation.

The feed and permeate solutions were recirculated during all experiments at flow rates of 175 and 50 L/h, respectively. The electrode solution was re-circulated over both electrode compartments from a single supply vessel at a flow rate of 50 L/h for experiments 1–3 and 74 L/h for experiments 4–10. The experimental conditions are summarized in Table I. The feed concentration (c_f), the feed resistance (R_f), the electrode- and permeate resistance (R_e), the membrane resistance (R_m), and the overall potential drop (ΔV_{tot}) were varied to investigate the effect of each on the transport rate of charged bioactive fragments to the permeate solution.

During the experiment the pH of the feed solution was maintained at pH 8.0 ± 0.5 by titration with 0.2 *N* NaOH (Merck, Darmstadt, Germany). The pH of the permeate solution was maintained at pH 4.0 ± 0.5 by addition of 0.2 *N* HCl (pa, BDH Laboratory Supplies, Poole, UK). The pH of the electrode solution was not adjusted. At the start of each run the permeate and electrode compartment contained a solution of 20 or 50 m*M* Na_2SO_4 (pa, Merck, Darmstadt, Germany) in demineralized RO water.

Analyses

Analytical RP-HPLC of the concentrate and permeate samples was carried out under the conditions reported previously (Recio and Visser, 1999). The composition of the α_{s2}-casein isolate was determined by the RP-HPLC method described by Visser et al. (1991). For quantification of the C-terminal peptide α_{s2}-CN f(183–207), a calibration curve of the peptide, chromatographically purified to high purity according to the procedure described by Recio and Visser (1999), was used.

Mass determination of the peptides in the permeate solution was performed on a Waters HPLC system connected on-line to a Quattro II triple-quadrupole instrument (LC-MS) (Micromass, Cheshire, UK) as described elsewhere (Recio and Visser, 1999) with some modifications. Peptides were eluted using a Widepore C_{18} 250 × 4.6 mm column (Bio-Rad Laboratories, Richmond, CA) with a linear gradient of solvent B in A going from 0% to 36% in 50 min at a flow rate of 0.8 mL/min. Solvent A was a mixture of acetonitrile–water–trifluoroacetic acid (100:900:1, v/v/v) and solvent B contained the same components in a different ratio (900:100:0.8, v/v/v).

Peptides from the permeate fraction were manually collected from the analytical RP-HPLC and freeze-dried. Identification of these peptides was performed by electro-spray ionization-tandem mass spectrometry (ESI-MS/MS) using a Quattro II triple-quadrupole mass spectrometer (Micromass) as described previously (Recio and Visser, 1999).

Calculation Procedures

The electrical field strength E_j in a compartment can be calculated from the conductivity of the solution in that compartment σ_j, the measured current I, and the electrode area A according to:

$$E_j = \frac{I}{\sigma_j \cdot A} \cdot 10 \qquad (2)$$

It is assumed that all solutions in the system were ideally mixed. The potential drop ΔV_j over each individual com-

Table I. Experimental conditions.

Experiment no.	ΔV_{tot} [V]	Initial cs_e, cs_p [m*M* Na_2SO_4]	Feed type	c_f [g hydrol./L]	IEX position	Vol_e [L]
1	40	20	A	2.4	Alternative[b,c]	1
2	40	20	A	2.4	Alternative[b,c]	10
3	60	20	A	2.4	Alternative[b,c]	10
4	40	20	A	2.4	Alternative[b]	10
5	20	20	D	2.0	Alternative[b]	10
6	40	20	D	2.0	Alternative[b]	10
7	20	50	D	2.0	Alternative[b]	10
8	40	50	D	0.8	Alternative[b]	10
9	20	20	D	2.0	Conventional[a]	10
10	40	20	D	2.0	Conventional[a]	10

[a]AMX membrane between anode and feed compartments and CMX membrane between cathode and permeate compartments.

[b]AMX membrane between cathode and permeate compartments and CMX membrane between anode and feed compartments.

[c]The compartment containing the anode as split into two compartments by addition of a second CMX membrane.

partment is found by multiplying the field strength in that compartment by the compartment thickness d_j.

The membrane-related resistance (the resistances of all membranes and their boundary layers) is calculated from the resistances of the solutions and the total current and applied potential difference, using Ohm's law:

$$R_m = \frac{\Delta V_{tot} - \Delta V_f - \Delta V_e - \Delta V_p}{I} \quad (3)$$

The cumulative electrical field strength in the feedstock compartment during an experiment is approximated by summation of the average driving force (calculated from Eq. (2)) during each time interval multiplied by the duration of the interval over all time intervals. Similarly, the cumulative energy consumption is estimated by summation of $\Delta V_{tot} \cdot I \cdot \Delta t$.

RESULTS AND DISCUSSION

Selectivity of EMF and UF

With EMF, slightly more than 10 components are selectively isolated from the feed (see Figs. 3 and 4). As expected, all identified peptides show a net positive charge at pH 7.0 (see Table II) and are proven or anticipated (on the basis of their positive charge) bioactive peptides. Six out of the 10 identified peptides (see Table II) have been found previously in antibacterial fractions from an α_{s2}-casein hydrolysate obtained after cation-exchange chromatography (Recio and Visser, 1999). Peptide α_{s2}-CN f(183–207), the target peptide, is clearly the predominant component in the EMF permeate (see Table II and Fig. 3). This peptide exhibits potent antibacterial activity against Gram-positive and Gram-negative microorganisms and its activity is related to its high net positive charge (Recio and Visser, 1999). The relative content of α_{s2}-CN f(183–207) increased from 7.5% in the feed solution to 25% (at maximum) in the permeate product (based on the ratio of peak areas). Furthermore the relative content increased with time. Longer operation times may therefore lead to an even higher product purity for α_{s2}-CN f(183–207). Peptide α_{s2}-CN f(164–179) also shows antibacterial properties, but is less active than α_{s2}-CN f(183–207) (Recio and Visser, 1999). Moreover, other peptides included within the domains of α_{s2}-CN f(183–207) and α_{s2}-CN f(164–179), such as α_{s2}-CN f(183–206) and α_{s2}-CN f(164–174), and a peptide with an oxidized methionine, α_{s2}-CN f(183–207)[c] are also expected to exhibit antibacterial activity. Oxidized forms of methionine-containing peptides were also observed during the isolation of lactoferricin-B from a lactoferrin hydrolysate (Bargeman et al., 2000) with EMF. Possibly the presence of oxygen, formed at the anode of the EMF module, causes oxidation of this amino acid.

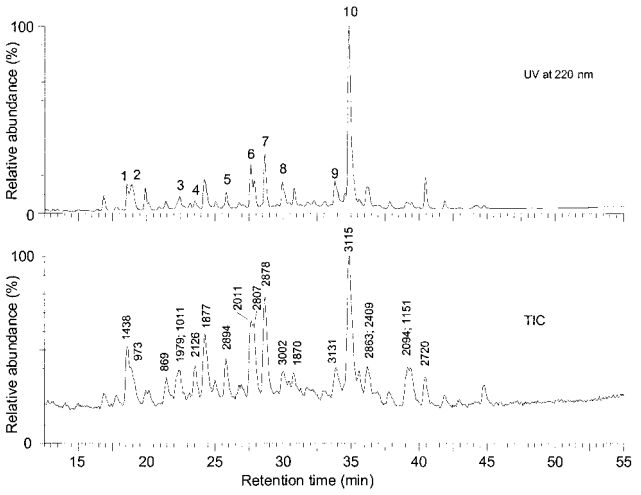

Figure 3. HPLC-MS analysis of the product obtained after 240 min of EMF experiment 3 (see Table II). The UV chromatogram and the total ion current (TIC) are shown. The masses determined are shown above the various peaks on the TIC profile. The peaks subjected to electrospray ionization–tandem mass spectrometry are indicated with numbers on the UV chromatogram.

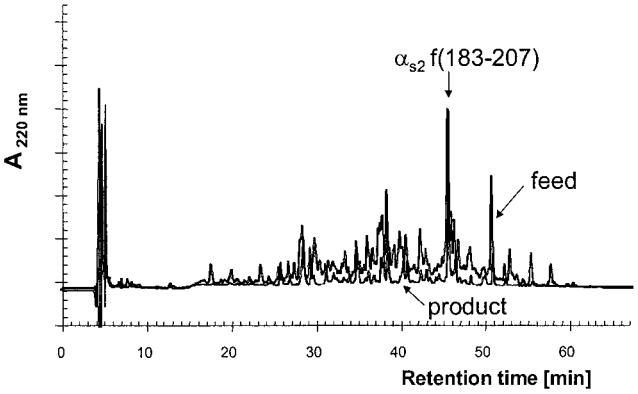

Figure 4. Analytical RP-HPLC chromatograms of feed and permeate after 240 min of EMF experiment 3 (see Table II).

In contrast to EMF, diafiltration with GR60PP resulted in high retention of bioactive peptides (see Fig. 5). The peak of α_{s2}-CN f(183–207) is almost absent in the chromatogram of the product and so are most of the other positively charged peptides identified. The low retention times of the peaks observed in the chromatogram suggest that the transported peptides are relatively small. The difference in selectivity is most likely not caused by differences in membrane fouling, since the water flux of the fouled membranes in both cases decreased to 30% of the initial clean water flux after 4 h of EMF and 3 h of diafiltration.

Consequently, in contrast to conventional ultrafiltration, EMF is, as expected, a selective process for the isolation of positively charged bioactive components from an α_{s2}-casein hydrolysate.

Table II. Molecular mass determination and peptide identification of the protein fragments obtained in the product compartment after 240 min of EMF experiment 3 (see Table I for experimental conditions).

Peak	Observed mass	Calculated mass[a]	Sequence position	Net charge at pH 7.0	Amino acid sequence[b]
1	1438	1438.7	α_{s2}-CN f(164–174)	+4	LKKISQRYQKF[e]
2	973	973.1	α_{s2}-CN f(89–95)	+1	YQKFPQY[f]
3	1979	1979.3	α_{s2}-CN f(148–163)	+2	TKKTKLTEEEKNRLNF[e]
4	2126	2126.4	α_{s2}-CN f(147–163)	+2	FTKKTKLTEEEKNRLNF[e]
5	2894	2894.4	β-CN f(164–189)[c]	+2	SLSQSKVLPVPQKAVPYPQRDM[c]PIQA[f]
6	2011	2011.4	α_{s2}-CN f(164–179)	+4	LKKISQRYQKFALPQY[e]
7	2878	2878.4	β-CN f(164–189)	+2	SLSQSKVLPVPQKAVPYPQRDMPIQA[f]
8	3002	3002.6	α_{s2}-CN f(183–206)	+5	VYQHQKAMKPWIQPKTKVIPYVRY[e]
9	3131	3131.8	α_{s2}-CN f(183–207)[c]	+5	VYQHQKAM[c]KPWIQPKTKVIPYVRYL[f]
10	3115	3115.8	α_{s2}-CN f(183–207)	+5	VYQHQKAMKPWIQPKTKVIPYVRYL[e]

[a]Average mass values.
[b]α_{s2}-CN and β-CN sequences according to Brignon et al. (1977) and Ribadeau-Dumas et al. (1972), respectively.
[c]Oxidized methionine.
[d]Identified by electrospray ionization-tandem mass spectrometry.
[e]Identified by Recio and Visser (1999).
[f]Identified during this work.

Transport Rate of α_{s2}-CN f(183–207) During EMF

Hydrolysate Concentration

A 2.5-fold increase in the hydrolysate concentration in the feed (from 0.8 to 2.0 g/L) resulted in a 2.1-fold increase in the amount of α_{s2}-CN f(183–207) transported during 4 h of operation (see Fig. 6). This bioactive component, which was predominantly present in the product, is taken as marker peptide for the transport of charged bioactive components. A proportional increase of the transport rate with the concentration is expected (see Eq. (1)). However, as a result of the lower conductivity of the feed containing 0.8 g/L hydrolysate, the electrical field strength in the feed compartment (the driving force) after 1 h of batch operation was a factor 1.1 higher than for the 2.0 g/L hydrolysate solution. This slightly counteracted the positive effect of the higher concentration on the amount of α_{s2}-CN f(183–207) transported. When this effect is taken into account, the effect of the concentration increase on the increased amount of α_{s2}-CN f(183–207) transported is practically in line with the expected trend based on Eq. (1).

Conductivity of the Electrode and Permeate Solutions

In contrast to EMF at constant conductivity of the electrode solution (experiment 2, see Table I), the peptide transport stagnated when the conductivity of the electrode solution was allowed to fall from 3.7 to 1.0 mS/cm (see Fig. 7). This decrease was caused by salt transport from the electrode compartments to the feed and the permeate compartments. As a consequence, especially the membrane-related (electrical) resistance and the resistance of the electrode solution increased. This led to a strong reduction of the electrical field strength in the feed compartment (the driving force for

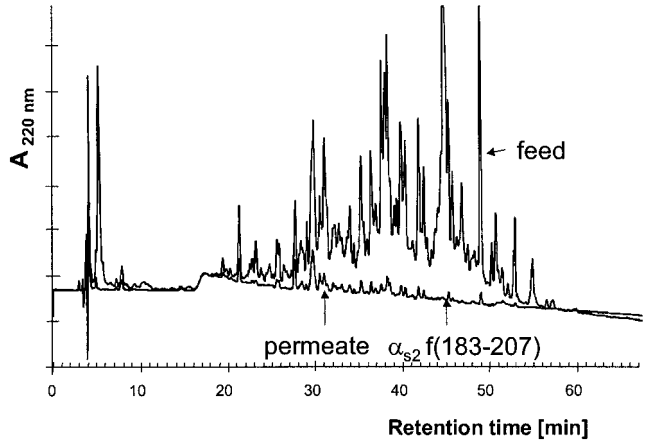

Figure 5. RP-HPLC chromatograms of feed and permeate during diafiltration on a GR60PP membrane at 170% DF.

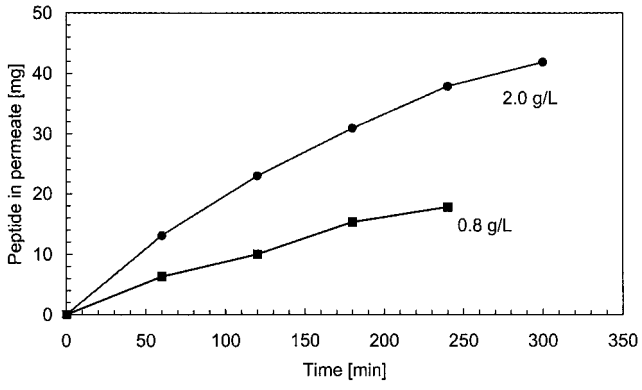

Figure 6. Effect of the hydrolysate concentration in the feed, c_f, on the amount of α_{s2}-CN f(183–207) peptide transported. Conditions: $\Delta V_{tot} = 40$ V, $cs_e = cs_p = 20$ mM Na_2SO_4 (initially), desalinated feed (D), alternative IEX membrane situation (experiments 6 and 8).

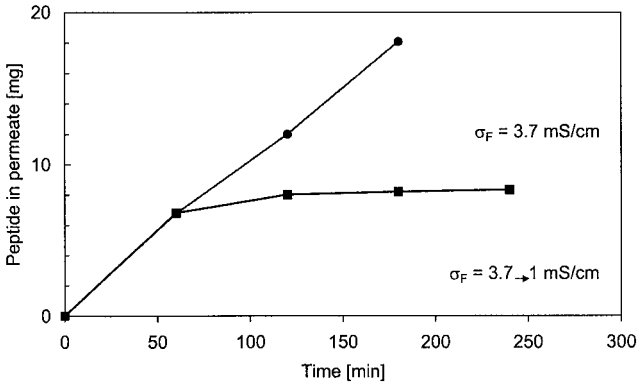

Figure 7. Effect of the decrease of the conductivity of the electrode solution on the amount of α_{s2}-CN f(183–207) peptide transported. Conditions: ΔV_{tot} = 40 V, cs_e = cs_p = 20 m*M* Na_2SO_4 (initial), feed A, alternative IEX membrane situation (experiments 1 and 2).

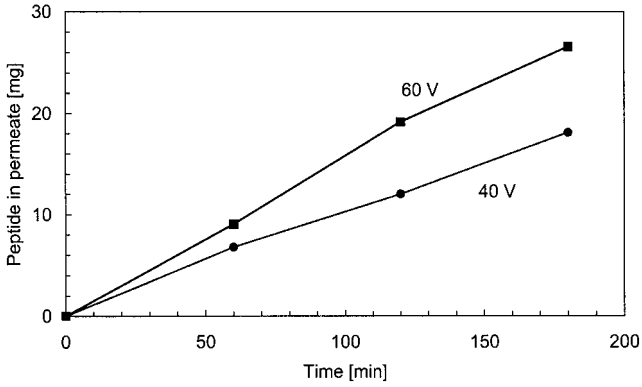

Figure 9. Effect of applied total potential difference on the amount of α_{s2}-CN f(183–207) peptide transported. Conditions: cs_e = cs_p = 20 m*M* Na_2SO_4, non-desalinated feed (A), alternative IEX membrane situation (experiments 2 and 3).

transport) from 1.1 to 0.2 kV/m and consequently the observed stagnation of peptide transport. A reduction of the conductivity of the electrode solution should therefore be avoided.

An increase in the conductivity of the electrode and permeate solutions as a consequence of an increase in the salt concentration from 20 to 50 m*M* Na_2SO_4 at 20 V overall potential difference did not affect the amount of α_{s2}-CN f(183–207) transported (see Fig. 8). This is in line with expectations because the calculated driving forces (electrical field strengths in the feed compartment) for both situations were equal.

Overall Potential Difference

An increase in the applied overall potential difference from 40 to 60 V resulted in a 1.4-fold increase of the total amount of α_{s2}-CN f(183–207) transported over 3 h (see Fig. 9). This is in line with the ratio of the calculated electrical field strengths in the feed compartment for 60 V over 40 V during the first hour of 1.3. Doubling the potential difference from 20 to 40 V resulted in a 2.5-fold and 3-fold increase of the amount of α_{s2}-CN f(183–207) transported after 3 and 4 h of EMF, respectively (see Fig. 10A, compare 20 V alternative with 40 V alternative). The maximum ratio of the calculated electrical field strengths in the feed compartment during these experiments of 2.2 (see Fig. 10B) was too small to explain the observed increases, especially the 3-fold increase. Possibly peptides were partly adsorbed to the membranes and the EMF equipment. This may have affected the amount of α_{s2}-CN f(183–207) transported, especially at low transport rates.

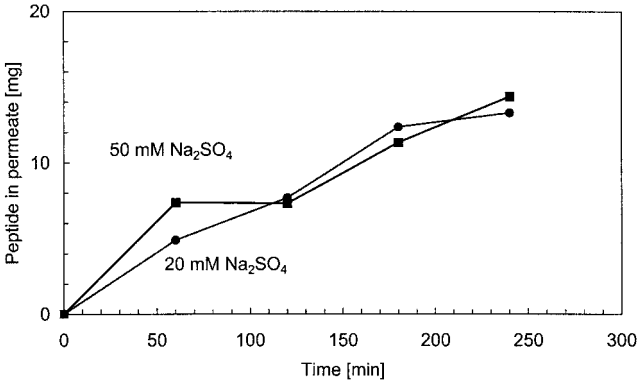

Figure 8. Effect of the initial conductivity of the electrode solution on the amount of α_{s2}-CN f(183–207) peptide transported. Conditions: ΔV_{tot} = 20 V, cs_e = cs_p (initial), desalinated feed D, alternative IEX membrane situation (experiments 5 and 7).

Conductivity of the Feed

The amount of α_{s2}-CN f(183–207) transported to the permeate could be increased by using a feed with a low conductivity (desalinated feed, see Fig. 11A). The average transport rate during 4 h of EMF was 1.2 g/m2 · h for the desalinated feed. Especially during the first hour of operation a higher amount of α_{s2}-CN f(183–207) was transported. However, after about 2 h the transport rates (the slope of the plotted lines) were equal, and consequently the difference in transport rates between a high-conductivity and low-conductivity feed for batch-wise EMF was small. The observed difference in the amount of α_{s2}-CN f(183–207) transported for both situations is partly explained by the difference in the electrical field strengths in the feed compartment (see Fig. 11B). Initially, this driving force for the desalinated feed was 2-fold higher than for the non-desalinated feed because of the high feed resistance. However, the ratio of these driving forces dropped considerably as the experiment progressed, and after 2 h the driving forces were practically equal. This is due to the relatively steep increase in the conductivity of the desalinated feed, as a result of salt transport from the electrode compartment to the feed compartment and consequently the relatively high reduction of the electrical resistance in this compartment. In-line desalination of the feed may therefore have a significant positive effect on the transport rate.

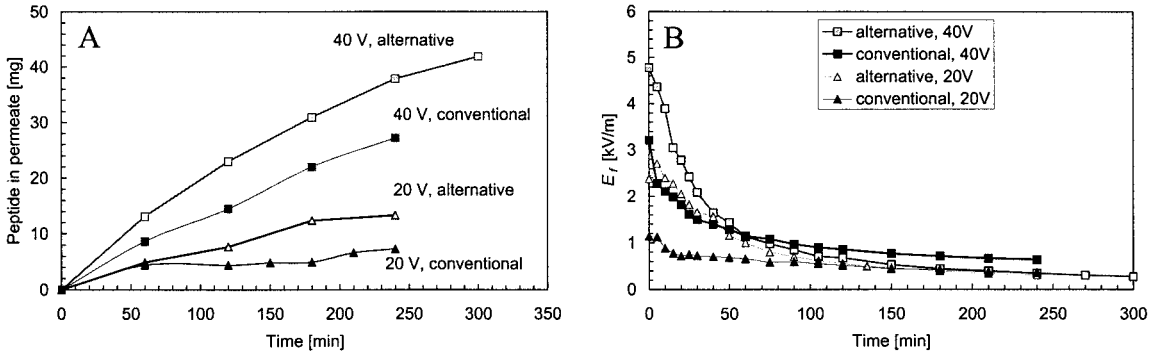

Figure 10. Effect of the arrangement of IEX membranes on the amount of α_{s2}-CN f(183–207) peptide transported (A) and the electrical field strength in the feed compartment (B). Conditions: $cs_e = cs_p = 20$ mM Na_2SO_4 (initial), desalinated feed (D) (experiments 5, 6, 9, and 10).

The amount of α_{s2}-CN f(183–207) transported as function of the cumulative driving force is shown in Fig. 12. For the desalinated feed, the transport of the α_{s2}-CN f(183–207) peptide initially required a considerably higher cumulative electrical field strength in the feed compartment than for non-desalinated feed: for the transport of 15 mg of α_{s2}-CN f(183–207) to the permeate, the required cumulative electrical field strength in the feed compartment, $\Sigma[E_f \cdot \Delta t]$, was approximately 10,000 kV · s/m for desalinated feed and 6,000 kV · s/m for non-desalinated feed. Since the α_{s2}-CN f(183–207) concentrations of both feeds were similar, this difference in the total amount of α_{s2}-CN f(183–207) in the permeate (equivalent to the cumulative α_{s2}-CN f(183–207) flux) is ascribed to the difference in electrophoretic mobility (see Eq. (1)). The relatively low initial electrophoretic mobility for the desalinated feed is attributed to the relatively low concentration of counter-ions required for α_{s2}-CN f(183–207) transport, resulting in retardation of the α_{s2}-CN f(183–207) transport rate. From a cumulative electrical field strength of 10,000 kV · s/m onward, the slopes of the lines (see Fig. 12) are practically the same, suggesting a similar electrophoretic mobility for both cases from that point on. This is due to the relatively steeper increase in the salt concentration (indicated by the conductivity) of the desalinated feed and is in line with the similar transport rates, as observed experimentally after 2 h.

Consequently, the anticipated advantageous effect of the high electrical field strength on the transport rate for low-conductivity feeds is partly counteracted by the low electrophoretic mobility of the α_{s2}-CN f(183–207) peptide. Nevertheless operation with a low-conductivity feed still results in a higher transport rate as mentioned earlier.

Position of the AMX and CMX Membranes Relative to the Electrodes

EMF with the CMX membrane separating the anode and the feed compartments and the AMX membrane separating the cathode and the permeate compartments (alternative situation) resulted in an increase of the amount of α_{s2}-CN f(183–207) transported during 4 h operation compared to operation with the AMX membrane separating the anode and the feed compartments and the CMX membrane separating the cathode and the permeate compartments (conventional situation). The ratio of the amounts transported was 1.5 during the entire experiment for EMF at 40 V and between 1.2 and 2 for an applied potential difference of 20 V (see Fig. 10A).

The lower initial transport rate for the conventional situation is in line with the lower driving force at the start of the experiment (see Fig. 10B). This lower driving force for the conventional situation was due to higher membrane-related resistances, probably caused by more pronounced limiting-

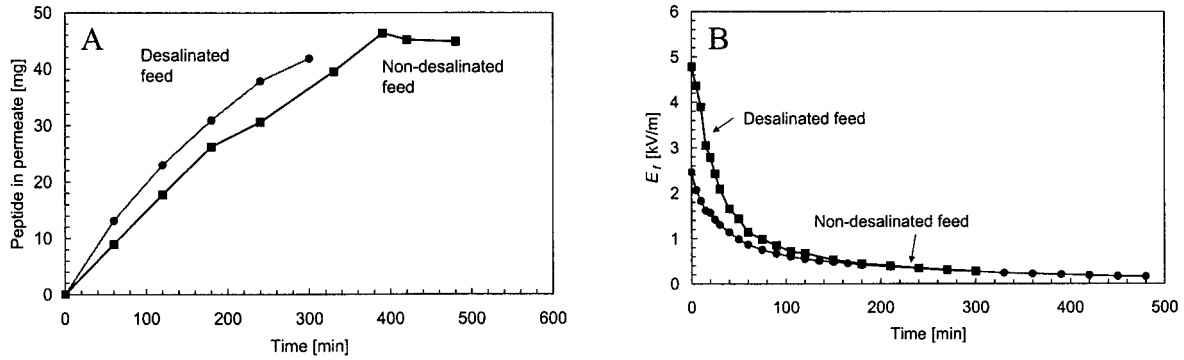

Figure 11. Effect of prior desalination of the feed on the amount of α_{s2}-CN f(183–207) peptide transported (A) and the electrical field strength in the feed compartment (B). Conditions: $\Delta V_{tot} = 40$ V, $cs_e = cs_p = 20$ mM Na_2SO_4 (initial), non-desalinated feed (A) and desalinated feed (D), alternative IEX membrane situation (experiments 4 and 6).

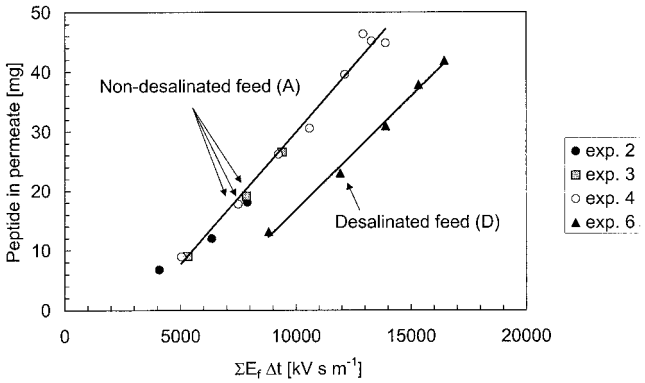

Figure 12. Amount of α_{s2}-CN f(183–207) peptide transported as a function of the cumulatively applied driving force (experiment numbers refer to Table I).

current effects (van Nunen, 1997). Due to the relatively low current, the salt transport from the electrode compartment to the feed compartment was relatively slow for the conventional situation. This resulted in a slower increase of the feed conductivity. Consequently the electrical field strength in the feed compartment exceeded that for the alternative situation after 1 h of operation. Despite this higher electrical field strength the transport rate for α_{s2}-CN f(183–207) did not exceed that for the alternative situation. This may be due to the relatively small increase of the concentration of the counter-ions in the feed compartment leading to a relatively low electrophoretic mobility for the conventional situation.

Observed Membrane-Related Resistances

The membrane-related (electrical) resistances ranged between 50% and 80% of the total resistance for all experiments. They were more than a factor 80 higher than the resistances reported for the IEX membranes alone (Perry, 1984), even for experiments where the current was below the limiting current (e.g., for experiment 2, where the measured current of 0.55 A was marginally below the limiting current $I_{\text{lim}} = 0.60$ A of the CMX membrane estimated on the basis of the correlations proposed by van Nunen (1997)). Furthermore, the electrical resistance of the UF membrane is estimated to be below a few ohms (from experimental data). The high membrane-related resistances are consequently not caused by the occurrence of limiting currents or the resistance of the UF membrane. On the basis of a visual inspection of the EMF module the most likely explanation is that a thin stagnant liquid zone is present in our exploratory equipment between one of the IEX membranes and its support. In this stagnant zone the mass transport of salts is relatively slow and governed by diffusion. Consequently depletion of salts may occur, resulting in a low conductivity and a high (membrane-related) resistance in this region. Because high membrane-related resistances reduce the electrical field strength in the feed compartment (the driving force for transport), the transport rates obtained may therefore be improved considerably by improving the design of the EMF module.

Effect of Process Parameters on Energy Efficiency

The energy required per milligram α_{s2}-CN f(183–207) transported depended on the process conditions applied (see Fig. 13). For EMF at 40 V potential difference with desalinated feed, the observed energy consumption per mg of α_{s2}-CN f(183–207) transported was lower than for EMF with non-desalinated feed (see Fig. 13, compare experiment 6 and experiment 4). This lower energy consumption is due to the relatively high α_{s2}-CN f(183–207) transport rate for the desalinated feed caused by a relatively high electrical field strength in the feed compartment in combination with a relatively low current and salt transport. The relatively low current was due to the relatively high electrical resistance of the feedstock. Thus little energy was wasted on salt transport. To achieve this energy advantage, the feedstock has to be desalinated. The costs of this desalination procedure have to be incorporated in process cost evaluations to determine the optimal process line-up.

The energy consumption per milligram α_{s2}-CN f(183–207) transported for the conventional IEX membrane situation was practically the same (marginally lower) as for the alternative IEX membrane situation (see Fig. 13, compare experiment 10 and experiment 6). Although the current was small and consequently relatively little salt was transported in the conventional situation, the transport rate of α_{s2}-CN f(183–207) was also relatively low due to the lower electrical field strength in the feed compartment (initially) and the lower electrophoretic mobility.

For non-desalinated feed a higher applied overall potential difference (60 V vs. 40 V) resulted in a higher energy consumption per milligram α_{s2}-CN f(183–207) transported (see Fig. 13, compare experiment 2 and experiment 3). Because the overall resistance of the EMF module was practically the same for both situations, the current was approxi-

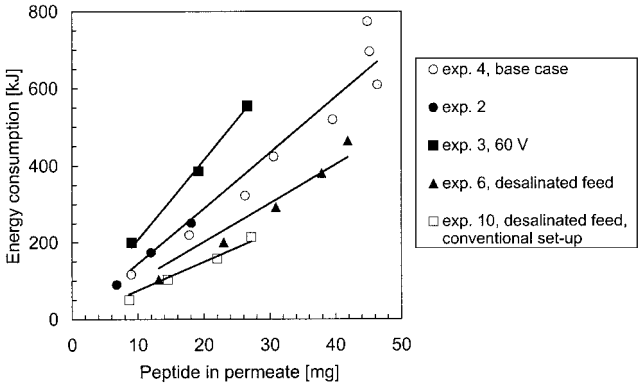

Figure 13. The energy consumption as function of the amount of α_{s2}-CN f(183–207) peptide transported. Starting point is experiment 4, using $\Delta V_{\text{tot}} = 40$ V, $cs_e = cs_p = 20$ mM Na_2SO_4 (initial), non-desalinated feed and the alternative membrane situation. Only deviations from this starting point have been indicated in the legend of the figure.

mately 1.5 times higher for operation at 60 V. In combination with the 1.5 times higher potential difference applied, this resulted in higher energy consumption (by a factor of about 2.3). The amount of α_{s2}-CN f(183–207) transported was only increased by a factor of 1.4, mainly as a consequence of the higher potential difference in the feed compartment. For operation at higher potential difference the transport rate of α_{s2}-CN f(183–207) is therefore increased at the expense of the higher energy consumption.

The energy consumption is relatively high for all situations. This is due to the high membrane-related resistances (between 50% and 80% of the total electrical resistance) caused by the presence of a small stagnant zone in the present EMF module and the relatively high thickness of the electrode and permeate compartments. Reduction of these resistances will have a positive effect on the energy consumption (reduction of the applied potential difference for the same current) and/or the transport rate (increase of the electrical field strength in the feed compartment for the same applied potential difference).

With respect to the economics of the EMF process optimization of the capital investment (transport rate) and the energy consumption per unit α_{s2}-CN f(183–207) produced is necessary. When the costs per square meter of membrane area (i.e., the costs of the equipment and the membranes) or the costs per square meter of electrode area are predominant, a high voltage is the preferred choice. However, when the energy costs are predominant, a low potential difference and possibly operation with desalinated feed (depending on the desalination costs) will be beneficial.

CONCLUSIONS

With batch-wise electro-membrane filtration (EMF) positively charged peptides are transported from the α_{s2}-casein hydrolysate feed to the permeate, whereas negatively charged or neutral peptides are retained. The predominant component in the permeate product, α_{s2}-CN f(183–207), is a peptide with proven potent antimicrobial activity against Gram-positive and Gram-negative microorganisms. The relative content of this bioactive target peptide is increased from 7.5% in the feed to 25% (at maximum) in the permeate product. Furthermore, most other peptides recovered in the permeate are proven or anticipated valuable bioactive peptides. In contrast, conventional pressure-driven diafiltration using the same ultrafiltration membrane, GR60PP, does not result in the isolation of this target peptide. Hence, the presence of the electrical field strength is essential for the isolation of positively charged bioactive peptides.

The maximum average α_{s2}-CN f(183–207) transport rate achieved at present is 1.2 g/m^2 · h. Since only the positively charged peptides are transported and convection is minimized during EMF, the transport rate is governed by electrophoretic transport. The transport rate should consequently be influenced by the electrical field strength in the feed compartment, the electrophoretic mobility, and the feed concentration. The results from this study indicate that the transport rate during EMF can indeed be increased by increasing the feed concentration, the overall potential difference or the conductivity of the electrode and permeate solutions or by decreasing the conductivity of the feed (by desalination of the feed). Furthermore, the position of the anion-exchange and cation-exchange membrane relative to the anode and cathode affects the transport rate of α_{s2}-CN f(183–207).

The results also indicate that the energy efficiency of EMF can be improved by operating at a relatively low overall potential difference and by the use of a low-conductivity (desalinated) feed.

Since the membrane-related resistances contributed 50–80% of the total electrical resistance and the feed concentration can be further increased, a considerably lower energy consumption and higher transport rates seem feasible after further optimization of the EMF module and the process conditions.

Daniëlle Stoffels, Narda Janssen, Charles Slangen, Jan Leenders, and Roelie Holleman are gratefully thanked for their contributions to the experimental and analytical work.

NOMENCLATURE

A	membrane or electrode area	[m^2]
c	concentration in the bulk solution	[mol/L] or [g/L]
c_f	feed concentration	[g/L]
c_s	salt concentration	[mol/L]
d	thickness of compartment	[m]
D	diffusion coefficient	[m^2/s]
E	electrical field strength	[V/m]
F	Faraday's constant (9.6×10^4)	[C/mol]
I	electrical current	[A]
J	transport rate	[g/m^2 · s]
k	convective coupling coefficient	[–]
R	resistance	[Ω]
t	time	[s]
u	electrophoretic mobility	[m · mol/N · s]
V	potential (difference)	[V]
Vol	volume compartment, supply vessel and piping	[L]
v	velocity	[m/s]
x	distance	[m]
z	charge	[mol charge/mol]

Greek Symbols

Δ	difference	[–]
Φ	flow rate	[L/h]
σ	conductivity	[mS/cm]
Σ	summation	[–]

Superscripts and Subscripts

b	bulk
e	electrode
f	feed
i	component index, interface
j	compartment index
m	membrane related
p	permeate
tot	total

References

Bargeman G, Dohmen-Speelmans M, Recio I, Timmer M, van der Horst HC. 2000. Selective isolation of high-value dairy components by electro-membrane filtration. Lait 80:175–186.

Brignon G, Ribadeau-Dumas G, Mercier J-C, Pélissier J-P, Das BC. 1977. Complete amino acid sequence of bovine α_{S2}-casein. FEBS Lett 76: 274–279.

Daufin G, Kerhevé FL, Aimar P, Mollé D, Leonil J, Nau F. 1995. Electrofiltration of solutions of amino acids or peptides. Lait 75:105–115.

Gill I, Lopez-Fandina R, Jorba X, Vulfson EN. 1996. Biologically active peptides and enzymatic approaches to their production. Enzyme Microb Technol 18:162–183.

Lentsch S, Aimar P, Orozco JL. 1993. Enhanced separation of albumin–poly(ethylene glycol) by combination of ultrafiltration and electrophoresis. J Membr Sci 80:221–232.

Lim S, Manusu HP, Gooley AA, Williams KL, Rylatt DB. 1998. Purification of monoclonal antibodies from ascitic fluid using preparative electrophoresis. J Chromatogr A 827:329–335.

Meisel H, Schlimme E. 1996. Bioactive peptides derived from milk proteins: ingredients for functional foods? Kiel Milchwirtsch Forschungsber 48:343–357.

Perry RH, Green D. 1984. Perry's chemical engineer's handbook. New York: McGraw Hill. p 17–41.

Pupanat L, Rios GM, Joulié R, Persin M, Pourcelly G. 1998. Electronanofiltration: a new process for ion separation. Sep Sci Technol 33:67–81.

Radovich JM, Behnam B. 1983. Concentration ultrafiltration and diafiltration of albumin with an electric field. Sep Sci Technol 18:215–222.

Recio I, Visser S. 1999. Identification of two distinct antibacterial domains within the sequence of bovine α_{s2}-casein. Biochim Biophys Acta 1428:314–326.

Rios GM, Freud P. 1991. Design and performance of ceramic EUF process for protein concentration. Key Eng Mater 61–62:255–260.

Rios GM, Rakotoarisoa H, Tarado de la Fuente B. 1988. Basic transport mechanisms of ultrafiltration in the presence of an electric field. J Membr Sci 38:147–159.

Ribadeau-Dumas B, Brignon G, Grosclaude F, Mercier J-C. 1972. Primary structure of bovine β casein. Complete sequence. Eur J Biochem 25: 505–514.

Robinson CW, Siegel MH, Condemine A, Fee C, Fahidy TZ, Glick BR. 1993. Pulsed-electric-field cross-flow ultrafiltration of bovine serum albumin. J Membr Sci 80:209–220.

Schlögl R. 1966. Membrane permeation in systems far from equilibrium. Ber Bunsenges Phys Chem 70:400.

Straatsma J, Bargeman G, van der Horst HC, Wesslingh JA. 2002. Can nanofiltration be fully predicted by a model? J Membr Sci 198: 273–284.

van der Horst HC, Timmer JMK, Robbertsen J, Leenders J. 1995. Use of nanofiltration for concentration and demineralization in the dairy industry; model for mass transport. J Membr Sci 104:205–218.

van Nunen CAMP. 1997. Design of a large-scale membrane-electrophoresis module for separation of proteins. Ph.D. thesis. Eindhoven, The Netherlands: Eindhoven University of Technology.

Visser S, Slangen CJ, Rollema HS. 1991. Phenotyping of bovine milk proteins by reversed-phase high-performance liquid chromatography. J Chromatogr 548:361–370.

von Zumbusch P, Kulcke W, Brunner G. 1998. Use of alternating electrical fields as anti-fouling strategy in ultrafiltration of biological suspensions: introduction of a new experimental procedure for cross-flow filtration. J Membr Sci 142:75–86.

Vreeman HJ, van Riel JAM. 1990. The large-scale isolation of α_{s2}-casein from bovine casein. Neth Milk Dairy J 44:43–48.

Wakeman RJ. 1998. Electrically enhanced microfiltration of albumin suspensions. Trans IChemE 76:53–59.

Yukawa H, Shimura K, Suda A, Maniwa A. 1983. Cross-flow electro-ultrafiltration for colloidal solution of protein. J Chem Eng Jpn 16: 305–311.